Review of Contemporary Philosophy
ISSN: 1841-5261, e-ISSN: 2471-089X
Vol 23 (02), 2024
pp. 7705 - 7726

mRNA Expression of Extracellular Matrix Proteins in Renal in vitro Models of Metabolic Acidosis and Hyperglycaemia

Abdullah R Alrasheed[1], Abeer Abdullah Asiri[2], Abdulrahman I Aljasser[3], Abdulaziz F alsharif[1], Dana H Alanazi[4], Abdullah A. AlHokair[5], Abdullah A. Binshalhoub[5], Sultan A. Alraqqas[6], Anas AAlshammari[1], Saleh H Alotaibi[7], Fahad Alzahrani[8], Areej I Aljasser[1]

[1] Assistant Deputyship of Preventive Health, Ministry of Health, Kingdom Saudi Arabia

[2] King Fahad Medical City, Riyadh second health cluster, MOH

[3] Diriyah hospital, Riyadh third health cluster, MOH

[4] Branch of the ministry of health in Riyadh Region

[5] General Department of Health Facilities Licensing

[6] Deputyship of Public Health, Ministry of Health, Kingdom Saudi Arabia

[7] Al Quwayiyah hospital, Riyadh first health cluster, MOH

[8] Director of Expatriates Examination program and travel health, MOH

Corresponding:

Areej I Aljasser,
Assistant Deputyship of Preventive Health,
Ministry of Health, Kingdom Saudi Arabia
dr.aljasser@hotmail.com

ABSTRACT: **Introduction**: Extracellular matrix proteins (ECM) deposition has been associated with tubulointerstitial fibrosis, leading to end-stage renal failure (ESRF). Several factors cause the extreme synthesis of ECM in the kidneys, including diabetes and metabolic acidosis. However, the detailed mechanisms leading to abnormal accumulation of ECM remain to be elucidated. **Aim:** To determine the effect of acidosis and hyperglycaemia on mRNA expression of MMP-2, MMP-9, collagen 1α1, collagen 4α1, TIMP1, and PAI-1 in renal proximal tubular epithelial cell (RPTEC). **Method**: RPTEC (HK-2) cells were cultured in 10% FCS-supplemented growth medium in 6-well plates until 80% of confluency was reached. Following this, cells were growth arrested for 24h in a serum-free medium and then exposed to **acidosis** (pH 6.7) or **hyperglycaemia** (25mM D-glucose, 30mM D-glucose) with separate controls for 24h and 72h, respectively. The

cells were then harvested, and total RNA was isolated. The mRNA was converted to cDNA, and the expression of the target genes was quantified using qRT-PCR. GAPDH was used for expression of gene expression analysis, and the ΔΔCt method was used to present the gene expression in terms of fold change. **Result**: Acidosis increased the mRNA expression of all ECM proteins; however, only the PAI-1 mRNA expression significantly increased. In hyperglycaemia, variable mRNA expression of the ECM proteins was measured over 72 hours. **Conclusion**: This study has shown that acidosis affects RPTEC as it increases the accumulation of all markers, which may lead to tubulointerstitial fibrosis. Hyperglycaemia had a variable effect on the expression of the ECM genes, suggesting that hyperglycaemia may lead to an increase in the deposition of ECM and then renal failure.

Keywords: Matrix Proteins, Renal, Metabolic Acidosis, Hyperglycaemia

Received: 22 July 2024 **Received:** 10 Sep 2024 **Accepted:** 18 Sep 2024

1. Introduction

Renal disease is a complex disease mediated by numerous mechanical, toxic, metabolic, and immunological factors [1]. These factors affect the kidney's tubulointerstitium, vasculature, and glomerulus, leading to CKD, one of the world's largest disease threats. CKD starts with loss of kidney function and ends with ESRF, or acute kidney disease, which can only be treated by long-term dialysis or kidney transplantation. ESRF exhibits a fibrotic abrasion affecting each section: glomerulosclerosis, vascular sclerosis, and tubulointerstitial fibrosis.

Tubulointerstitial fibrosis (TIF) is a condition where the connective tissue has been deposited detrimentally on the kidney parenchyma [2]. This progression occurs as a result of CKD, and all patients with this progression express a lessened renal function with time. TIF has been associated with abnormal ECM synthesis and degradation, which may cause an accumulation of ECM. ECM synthesis is part of the regular repair progression after any damage, but the extreme synthesis of the extracellular matrix is detrimental [1].

Metabolic acidosis is portrayed through a crucial decline in the serum consistency of bicarbonate (HCO3–), a consequential reduction in the arterial partial pressure of carbon dioxide (PaCO), and a decrease in blood pH [3]. The incidence of chronic metabolic acidosis might progress with the predictable increase in CKD in our maturing population. Metabolic acidosis -acute or chronic- can have essential unfavourable effects on cellular function and can lead to raised morbidity and mortality [4]. It has been confirmed that metabolic acidosis in

animals and humans is a risk factor for CKD progression [3].

Hyperglycaemia is a risk factor for diabetic nephropathy leading to ESRE. It is correlated with an increment in mesangial cell amplification and hypertrophy, as well as with expanded matrix production and basement membrane inspissation [5]. In addition, it influences glomerular hypertension and hyperfiltration, resulting in mechanical stress on the glomerular structures, and this motivates amplified transcription of transmuting growth factor–β1 (TGF-β1) composed with a reduced action of matrix-degrading metalloproteinases [6].

2. Theoretical Overview of the Main Concepts

Matrix metalloproteinases (MMPs) are a protein family that includes zinc-dependent proteases. These enzymes play a pivotal role in degrading and remodelling connective tissue constituents such as elastin, collagen, casein, and gelatin [7]. Furthermore, MMPs participate in cell-cell adhesion, cell-matrix adhesion, cell movement, stimulation, and release of cytokines and extracellular matrix-bond growth factors [8]. The kidney expresses, as a minimum, 10 MMPs (MMP-1, -2, -3, -9, -13, -14, -24, -25, -27 and -28) and their activation is managed by tissue inhibitors of metalloproteinases (TIMP), which is also exhibited from the kidney as TIMP-1, -2 and -3, together with other proteinase inhibitors, such as tissue factor pathway inhibitor-2 and α-2-macroglobulin [9]. It has been proven that MMP-9 and MMP-2 have a direct role in the stimulation and, thus, the complete progression of renal tubular cell epithelial-mesenchymal transition (EMT). These MMPs assist in this process by interrupting the integrity of the tubular cell membrane [10]. The process helps in migrating and accumulating the newly transmuted mesenchymal cells and fibrosis progression through ECM accumulation [8]. ECM accumulation is assisted by reduced MMP activity chiefly because of excessive production of TIMP. However, the reduction in the MMP synthesis also contributes to the ECM accumulation [11]. This illustrates that MMPs have a role in the kidney fibrosis.

3. Methodology

Cell culture

ECM mRNA expression was examined in immortalised human proximal tubular cell line HK-2 (ATCC, Teddington, UK; #CRL-2190) in order to ascertain the impact of acidosis and hyperglycemia. The cells were cultivated in a growth medium at 50:50 DMEM (Ham's F12) (Lonza #BE12-61F and Life Technologies; #11966) containing 5% foetal calf serum (FCS), 5 mM glucose, 50 μg/ml streptomycin, 20 mM HEPES 250 U/ml penicillin, and 5 mM glutamine in 5% CO_2 at 37 °C. The cells were then seeded at a pre-determined density of 4 x 10^4 cells/well onto the six-well culture plates. Following this, these cells were treated to a serum-free media

(1:1 mixture of Ham's F12 and DMEM) for 24 hours after reaching 85% confluency. After that, the cells were subjected to either acidosis or hyperglycemia.

Acidosis Model

After a single wash with 2 milliliters of sterile phosphate-buffered saline (PBS) (Lonza #BE17-517Q) per well, cells were then cultured in the serum-free medium (SFM) that was supplemented with either a 2% pH 7.4 solution Bis–Tris buffer consisting of 25% 0.625 M bis-Tris [Sigma-Aldrich, Dorset, UK, #B9754] and 75% 0.625 M bis-Tris HCl [Sigma-Aldrich, Dorset, UK, #B6032]) or a 2% pH 6.7 solution (5% 0.625 M bis-Tris and 95% 0.625 M bis-Tris HCl). After this, the cells were incubated at 37 °C for 24h.

Hyperglycaemia Model

The cells were washed with 2 millilitres of sterile phosphate-buffered saline (PBS) per well after reaching 85% confluency. Serum-free media (SFM) supplemented with either 30 mM, 25 mM and 5-, 25-, and 30-mM D-glucose (SIGMA #080M0182V) or a combination of 5 and 25 mM D-glucose L-glucose (Alfa Aesar #10127841) was then administered to them. The cells were then incubated for 24, 48, and 72 hours before being harvested, with the medium being changed every day.

Cells Harvesting and RNA Isolation

Acidosis Model

The culture medium was extracted from the wells of six-well plates, after which the cells were rinsed with 2 mm of ice-cold PBS. Following the manufacturer's directions, the Isolate II RNA Mini Kit (BioLine, UK) was utilized for cell extraction and RNA isolation. The cells were harvested in a lysate buffer of 350 µL total volume, consisting of 350 µL of RLY and 3.5 µL of beta-mercaptoethanol in each well. The resulting lysate was put into an Eppendorf tube. Following the vigorous vortexing of the lysate, it was transferred into a filter tube and placed within a collection tube containing 2 millilitres of liquid. After the Isolate II filter was removed and discarded post-centrifugation at 11,000 revolutions per minute for one minute, followed by the addition of 350 µL of 70% ethanol to the homogenized lysate. The mixture was then applied to Isolate II RNA Mini Column and centrifuged for thirty seconds at a speed of fifteen thousand revolutions per minute (RCF). After placing the column into a fresh 2-millilitre collecting container, 350 µL of membrane desalting buffer (MEM) was introduced. The column was centrifuged for one minute at 11,000 RCF, and 95 µl DNase I was added to the

centre of the silica membrane. The composition included 10 µl of reconstituted DNase I and 90 µl of DNase I reaction buffer for each isolation. Silica membrane was incubated at room temperature for 15 minutes. The sample underwent a washing procedure with wash buffer RW1 (200 µl) and was centrifuged for thirty seconds at a relative centrifugal force of 11,000 RCF. Thereafter, the sample underwent an additional wash with 600 µL of RW2 and centrifugation for 30s at 11,000 RCF. The column was removed from the collection tube and put into a 1.5 ml tube that was nuclease-free after being further cleaned with 250 µl of RW2. After that, the column was centrifuged for two minutes at 11,000 RCF of relative centrifugal force. After adding sixty µL of RNase-free water to the nuclease-free 1.5 ml collecting vial, it was centrifuged for one minute at 11,000 rpm. The NanoDrop 2000 or 2000c spectrophotometers or NanoDropTM One/OneC Microvolume UV-Vis Spectrophotometer, both manufactured by ThermoFisher Scientific in the UK, were used to measure the RNA concentration. Before being analyzed, the materials were separated into aliquots and stored at -80 °C.

Hyperglycaemia Model

Subsequent to the aspiration of the cells and the removal of the media from the wells of the 6-well plate, the cells were washed with ice-cold phosphate-buffered saline (PBS). Cells were harvested, and RNA was isolated utilizing the EZ-RNA II Total RNA Isolation Kit (devoid of chloroform), produced by BIOLOGICAL INDUSTRIES in Israel, in accordance with the manufacturer's guidelines. A 1.5-milliliter Eppendorf tube was then filled with the cell lysate. In conclusion, each well received 0.5 millilitres of denaturing solution. Before adding 0.4 millilitres of water-saturated phenol, the homogenate was allowed to come to room temperature and incubate for five minutes. 0.09 millilitres of 1-bromo-3-chloropropane (BCP) were added to the mixture following a vigorous vortexing of the liquid. The mixture was vortexed once again for fifteen seconds and then allowed to sit at room temperature for 10 minutes. The materials were inspected after being centrifuged for 10 minutes at 4 °C at 12,000 RCF. After moving the top phase to a fresh tube, the mixture was mixed with 0.5 millilitres of isopropanol. After carefully combining the ingredients, the mixture was incubated for 10 minutes at room temperature. To pellet the total RNA, the samples were centrifuged for 8 minutes at 12,000 RCF and 4 °C, followed by the collection of the supernatant. The RNA pellet was rinsed with one millilitre of 80% ethanol. Following five minutes of centrifugation at 7,500 RCF at 4 °C, the samples were aspirated to remove the ethanol. The RNA pellet was allowed to air dry before adding thirty µL of water treated with DEPC. The RNA concentration was determined using the spectrophotometer. The materials were separated into aliquots and kept at -80 °C before

analysis.

Reverse Transcriptase PCR

After defrosting the RNA samples on ice, they were subjected to vortexing and centrifugation for a brief duration. A Tetro cDNA Synthesis Kit, procured from BioLine in the United Kingdom, was employed to facilitate the conversion of cDNA. This was undertaken per the manufacturer's recommendations. In summary, 2 micrograms (μg) of RNA were transcribed for each sample analysed. To facilitate the transcription process, a precise sample volume and water exceeding 12 μl were introduced into a polymerase chain reaction (PCR) tube. Subsequently, eight μL of the master mix were added to each PCR tube. The master mix was composed of one microliter of primer oligo dT, one microliter of a ten millimolar dNTP mix, four μL of 5x RT buffer, one microliter of RiboSafe RNase inhibitor, and one microliter of Tetro reverse transcriptase. Both centrifugation and vortexing were conducted on the mélange for a short duration. The samples underwent a cycling protocol with the heated lid maintained at 112 °C following their transfer to the thermocycler (Q Cycler II, Biotron Healthcare, India). The program was implemented subsequent to the delivery of the samples. The samples underwent incubation at a temperature of 45 °C for thirty minutes, after which the process was stopped for 5 minutes at 85 °C. Samples utilized for the RT-PCR were preserved at a temperature of -20 °C prior to the execution of the qPCR.

Primers Test

Fourteen primer sets for both the extracellular matrix (ECM) and the housekeeping gene were acquired from Thermo Fisher (UK). The primer pairs were designed to anneal to independent exons, each separated by at least one intron. Table 1 presents the primer sequences that have undergone testing.

Table 1: Inventory of primers and their sequences.

Human Genes	Forward Primer	Reverse
Col Iα1	GTCGAGGGCCAAGACGAAGA	GTTGTCGCAGACGCAGATCC
Col IVα1	CGTCGTGCTGCTGCTGCT-	GCCCCTCAGGTCCTTGCAT
MMP-2 (A)	GCCAGGGAGCGCTACGA	GGGGCAGCCATAGAAGGTGTT

MMP-9	TTCGACGTGAAGGCGCAGAT	GGAACTCACGCGCCAGTAGA
TIMP1	CGCAGCGAGGAGTTTCTCAT	CTCTGCAGTTTGCAGGGGATG
PAI-1	CGAGGTGAACGAGAGTGGCA	CCCAGGGTCAGGGTTCCATC
GAPDH	GTGAGGACGGGCGGAGAGAAA	GGTGACCAGGCGCCCAATA
ß-Actin	CACAGAGCCTCGCCTTTGC	CCACGATGGAGGGGAAGAGC
RPS13	CTGACGACGTGAAGGAGCAG	AGGAAGATCAGGAGCAAGTCCC
GAPDH Ex 6 & 7	CATCCATGACAACTTTGGTATCG	TGGCAGGTTTTTCTAGACGG
MMP-2 (B)	CGCTACGATGGAGGCGCTAAT	CTCCTTGGGGCAGCCATAGA
MMP-2 (C)	GCTACGGAGGCGCTAAT	CTCTCCTTGGGGCAGCCATA
MMP-2 Ex 3 & 4	GACAGTGGATGATGCCTTTG	GTCCGTCCTTACCGTCAAAG
MMP-2 Ex 6 & 7	GCGACAAGAAGTATGGCTTC	GCGGTCATCGTAGTTGG

Col Iα1 = collagen Iα1; Col IV α1 = Collagen IV α1; MMP = Metalloproteinase; TIMP = Tissue inhibitor metalloproteinase; PIA-1 = Plasminogen activator inhibitor; GAPDH = Glyceraldehyde-3-phosphate dehydrogenase; RPS13 = Ribosomal protein S13.

A Q5® High-Fidelity PCR Kit, catalogue number E0555 (New England Biolabs, United States), was used to determine the primer products' abundance and molecular size, as directed by the manufacturer. In all, 11.51 µL of master mix, including 0.63 µL of 10 mM each forward and reverse primer; 5 µL of nuclease-free water; and 6.25 µL of Q5 high-fidelity 2X master mix, was discharged into each tube. In addition, each tube contained 0.5 µL of the template. The PCR vials were then placed in a Q-Cycler II thermocycler manufactured by Biotron Healthcare in India. The cycling protocol includes an initial denaturation phase at 98 °C for 30 seconds, followed by 35 cycles of denaturation at 98 °C for 10 seconds and annealing at 62 °C for 30 seconds for the remaining nine primers: Col 1, Col 4, MMP9, MMP-2 (A), TIMP-1,

PAI-1, GAPDH (A), α-Actin, and RSP13. The primers (GAPDH(B), MMP-2 B, C, Exons 3 and 4, and Exons 6 and 7) were annealed at 60°C for 30 seconds. The last extension phase was then carried out for four minutes at 72°C.

Agarose Gel Electrophoresis

A solution consisting of 0.5% Tris base, 0.1% glacial acetic acid, and 0.5 M EDTA was prepared to formulate a 1x Tris-acetate-ethylenediaminetetraacetic acid (TAE) running buffer, which was subsequently combined with 2% agarose gel. Prior to the cooling process, 6% of Midori Green (NIPPON Genetics EUROPE GmbH, Germany, #MG04) was incorporated into the concoction. After introducing the gel into the tank and allowing it to rest for approximately 45 minutes, TAE buffer was subsequently administered. The molecular weight reference was a Hyperladder (bp 25, BioLine, United Kingdom). 2µL of the 1x loading buffer, comprising 5% glycerol and 0.04% Orange G dye, were combined with the samples. Following the application of the samples, the gel was subjected to an operational voltage of 5 V/cm. The DNA bands were visualized and subsequently photographed under ultraviolet illumination (Syngene, United States).

Quantitative Real Time-PCR

After defrosting, the samples were amalgamated and subjected to brief centrifugation. Per the manufacturer's instructions, a SensiFAST™ SYBR® Hi-ROX Kit (Bioline, UK; # BIO-92005) was employed for quantitative polymerase chain reaction (qPCR). In summary, 2 µl of the RT-PCR samples were dispensed into each well of 96-well PCR plates following a dilution of 1:4 with DNase/RNase-free water. A total of 0.8 µl of 10 µM forward primer, 0.8 µl of 10 µM reverse primer, 6.4 µl of deionized water (H2O), and 10 µl of 2x SensiFAST SYBR Hi-ROX Mix were incorporated into 18 µl of the master mix. For each primer pair, the negative qPCR controls consisted of RT-PCR samples that utilized water in lieu of the template. Each sample and control underwent two separate examinations. After centrifugation and applying optical film sealing, the qPCR plates were dispatched to the Stratagene thermocycler Mx3000P. The subsequent phases constituted the qPCR protocol: The acidosis sample, which includes Col 1, MMP-9, Col 4, Timp-1, PAI-1, and α-Actin, underwent 40 cycles consisting of the following steps: i) denaturation at 95°C for 5 seconds, ii) annealing at 62°C for 10 seconds, with an additional annealing period of 15 seconds, and iii) extension at 72°C for 15 seconds. The standard for the melting curve protocol of the instrument was implemented for each quantitative polymerase chain reaction (qPCR) program. To assess the relative differences in

gene expression, the Ct values derived for each target gene were normalized against the corresponding Ct values of glyceraldehyde-3-phosphate dehydrogenase (GAPDH) and β-Actin, utilizing the ΔΔCT method. The averages for the reference gene and the marker duplicate samples were calculated. ΔCt value was expressed as the difference between the mean of the sample and the mean of the reference. Subsequently, the value of 2^-ΔCt was calculated, followed by the determination of its mean and standard deviation. The mean of the 2^ΔCt values for the treated samples was divided by the mean of the 2^-ΔCt values for the control sample in order to ascertain the ΔΔCt values.

Statistical analysis

In comparing two samples, the Statistical Package for the Social Sciences (SPSS, version 23) was used to analyse the statistical differences among multiple comparisons. This was achieved through either analysis of variance (ANOVA) accompanied by Tukey's post hoc analysis or the Student's t-test. The statistical significance of the P value ($P < 0.05$) was established as significant.

Results

Cell morphology in acidosis and hyperglycaemia model

The effect of acidosis on HK-2 cells was investigated under a light microscope (Figure 1). The morphology of the cells was similar in the acidosis condition (pH 6.7) to the control condition (pH 7.4), which means that acidosis did not have an apparent effect on the cell's morphology. However, the number of cells on day 1 appeared to be less than on day 0.

The cell's morphology of the HK-2 cells exposed to varying concentrations of glucose (Figure 2B: 25mM D-glucose, Figure 2C: 30mM D- glucose and Figure 2D: 5mM D-glucose + 25mM L-glucose) appeared similar to the control cells (Figure 2A) during the three days of treatment. However, the number of cells declined over 72 h compared to the number of cells at 0 h.

Expression of ECM and housekeeping genes in acidosis and hyperglycaemia models

Primers test

Nine primers (Col Iα1, Col 4α1, MMP-2, MMP-9, TIMP-1, PAI-1, GAPDH, β-Actin and RPS13) were tested, and only MMP-2 (A) and GAPDH (A) did not produce a visible band, as shown in Figure 3A. PCR was carried out with an annealing temperature of 60ºC for MMP-2 primers, and out of the three targets, no bands were observed (Figure 3B). Further primers of MMP-2 were purchased, as shown in Table 1, and PCR was run with an annealing temperature

of 60ºC, but none produced a visible band (Figure 3C). Therefore, MMP-2 was excluded from the experiment.

In addition, PCR was run to test another different sequence of GAPDH, namely GAPDH (B), because GAPDH (A) produced multiple bands when it was tested again (Figure 3D). GAPDH (B) showed a strong band with a molecular weight of about 260 bp (Figure 3D). Therefore, GAPDH (A) was discarded, and GAPDH (B) was used as a housekeeping gene in the qRT-PCR. Although the RPS13 housekeeping gene produced a visible band (Figure 3A), it was excluded from the experiment because this band was too strong.

Agarose electrophoresis of qPCR products

Agarose gel electrophoresis was run with the representative samples for each primer to confirm the results of the melting curve plots. Following the melting curve plots, Figure 4A and B show that the primers Col 1α1, Col 4α1, MMP9, TIMP1, PAI-1, GAPDH and β-Actin produce one visible. Furthermore, Col 4α1 reactions demonstrated the presence of more than one band, and β-Actin samples produced a smear. These results and the melting curves for Col 4α1 and β-Actin (Figure 4B and G) led to excluding these two targets from the qPCR data analysis.

All negative control samples did not produce any bands, except for a single TIMP-1 negative control in the hyperglycaemia model, indicating contamination of that sample with a template from a test sample.

mRNA Expression of fibrosis markers using in ΔΔCt method analysis

Acidosis Model

The investigation related to the impact of acidosis on the mRNA expression of the ECM markers (PAI-1 and Col 1α1), TIMP-1 and MMP-9 were investigated using quantitative real-time PCR (qPCR) and the ΔΔCt expression of these genes by assessing their expression in acidosis (pH 6.7) compared to normal pH (pH 7.4). Expression of these genes was normalised to GAPDH to obtain the ΔΔCt expression.

The mRNA expression of PAI-1 was significantly increased (~16-fold) by acidosis compared to pH 7.4 (Figure 5A). In addition, the mRNA expression of MMP-9 in (pH 6.7) the model raised approximately 4.5-fold compared to (pH 7.4) the model. Furthermore, Figure 5A shows that the mRNA expression of Col Iα1 increased ~5-fold while the expression of TIMP-1 mRNA increased ~6-fold in the acidosis condition compared to their expression in the control condition. However, all the increases were not significant.

Hyperglycaemia model

Investigation about the impact of hyperglycaemia on the mRNA expression of the ECM genes was made by comparing the three conditions of hyperglycaemia (25mM, 30mM and 5mM D-glucose + 25mM L-glucose) and the control condition (5mM D-glucose) at three different times (24h, 48h, and 72h). mRNA expression of Col 1α1 was increased by ~1.5-fold in the 30mM glucose at 24h and 1.9-fold at 72h, while it decreased at 48 h about -0.75 fold and also at 48h and 72h in the 25mM D-glucose concentration compared to control condition (Figure 6A, B and C). Additionally, Figures 7D, G, J, F, I, and L show that MMP-9, TIMP-1, and PAI-1 mRNA expression elevated approximately 2-fold at 24h and 72h. However, this increase in mRNA expression of all the genes was not statistically significant.

4. Discussion

Tubulointerstitial fibrosis occurs as a result of the excessive accumulation of excessive ECM, thereby preventing the effective repair of kidney damage. The mRNA expression of ECM components (collagen I alpha 1 type and PAI-1), MMP-9, and TIMP-1 can be used to evaluate the progression of kidney fibrosis. Collagen I is the principal fundamental protein in various tissues, and irregularities in collagen I production and structure correlate with several connective tissue disorders [12]. Healthy kidneys normally produce low amounts of PAI-1, but it is produced extensively in acute and chronic kidney disease. PAI-1 has been implicated as a moderator in several processes, including fibrosis [13]. Notably, it also regulates the adhesion or migration of cells, wound healing, angiogenesis, and tumour cell metastasis.

Furthermore, under normal conditions, MMP-2 and MMP-9 can be produced at low levels by the kidneys' mesangial and tubular epithelial cells. However, the mRNA expression of MMP-2 and MMP-9 was elevated during the progression of renal fibrosis [14], and acidosis was seen to affect the expression of PAI-1, collagen I, TIMP-1, and MMP-9 mRNA. It increased in all markers, while the mRNA expression values of all the predicted target genes were variable in the hyperglycaemia model.

Acidosis Model

Metabolic acidosis has been described as a consequence of, and also a contribution to, chronic kidney disease. It is believed that an increase in blood pH damages the kidney cells, producing ECM proteins. The production thereof can be excessive in some situations, which, in turn, results in end-stage renal failure (ESRF). An upregulation in the mRNA expression of PAI-1 and collagen I as a reaction to acidosis was demonstrated in the current study. PAI-1 is thought

to be a mediator in other processes besides the inhibition of fibrinolysis, including renal fibrosis. In addition, an increase in PAI-1 expression leads to an accumulation of ECM, ultimately causing chronic kidney disease [13]. According to [15], transforming growth factor-β (TGF-β) mediates the synthesis of PAI-1 and plasminogen activator. [16] found that PAI-1 expression increased when mice that overexpressed TGF-B developed glomerulosclerosis. Additionally, TGF-β can be induced by angiotensin II, which, in turn, leads to the stimulation of PAI-1 production [17]. [18] demonstrated that elevated intrarenal angiotensin II activity could be triggered by intrarenal or H^+ dietary acidosis through the renin-angiotensin system.

Furthermore, the accumulation of ECM components, including type I collagen, is a marker of tubulointerstitial fibrosis [19]. [19]. According to Poczatek et al. (2000), extreme pH conditions induce the activation of latent transforming growth factor-beta (TGF-β) through the proteolytic cleavage of the latency-associated peptide (LAP). This process modifies the interaction between LAP and the mature TGF-β domain. TGF-α has been recognized as a modulator of ECM accumulation due to its capacity to enhance the expression of ECM components such as collagen [20]. Thus, the upregulation of the mRNA expression of PAI-1 (~16 fold that of the control) and collagen type I (~5 fold that of the control) in this study suggests that this leads to an increase in ECM production, which then results in tubulointerstitial fibrosis.

MMPs also have the ability to degrade ECM proteins, including collagen, and contribute to the initialisation of the epithelial-mesenchymal transition (EMT) pathway, which leads to renal fibrosis, particularly MMP-9 [21]. [22] demonstrated that an increase in TIMP-1 expression led to renal interstitial fibrosis in an inflammatory way. A significant increase in mRNA levels of MMP-9 (~ 4 fold that of the control) and TIMP-1 (~6 fold that of the control) was observed in the current study. This is evidence of the contribution of acidosis to tubulointerstitial fibrosis.

Metabolic acidosis results from the elevation in net endogenous acid production, in that of the excretion of urinary or gastrointestinal HCO_3^-, or due to a reduction in renal HCO_3^- production. This indicates a decline in the excretion of NH^-_3 and net acid. The kidneys play a key role in ensuring the acid-base balance as they reabsorb the filtered HCO_3^- in the proximal tubule, excrete acid or alkali, and generate new forms of NH^-_3 and HCO_3^-. An association has been found between metabolic acidosis and tubulointerstitial fibrosis.

Metabolic acidosis induces renal injury through several mechanisms, including enhancing NH-3 synthesis [23], the activation of the substitute complement pathway, initiating inflammatory mediators, and alkalinization of the interstitial environment [24]. Elevated levels of intrarenal

ammonia enhance the C3b-like properties, specifically the production of C3 convertase, through interaction with the thioester bond in C3. C3 accumulates in the peritubules due to the subsequent activation of the substitution pathway. The membrane attack complex C5b-9 subsequently generates chemoattractants indicative of tissue injury [25, 26].

Increased endothelin (ET), an endothelial cell-derived peptide comprising three isoforms (ET-1, ET-2, and ET-3), correlates with acidosis, resulting in tubulointerstitial injury. The tubular and endothelial cells synthesise ET-1 in comparatively extreme quantities and have immense ET receptors [27, 28]. [29] illustrated that ET-1 stimulates fibronectin and collagen synthesis. In addition, the expression of renal ET-1 has been connected to proteinuria and glomerular levels, as well as tubulointerstitial injury [30]. ET is thought to manage several renal functions, such as the acid-base balance. ET-1 reacts to the systemic acid challenge by moderating elevated renal acid excretion [31].

All these studies illustrate that induction of acidosis in the kidney leads to tubulointerstitial inflammation and injury, while tubulointerstitial inflammation leads to excessive synthesis of the ECM, thereby causing renal fibrosis. This study also demonstrated that the mRNA expression of ECM (PAI-1 and collagen I), TIMP-1, and MMP-9 was elevated. Thus, acidosis may also contribute to tubulointerstitial fibrosis.

Hyperglycaemia Model

Diabetic nephropathy is a principal cause of ESRF, resulting in significant morbidity and mortality [32]. It is characterised by an increase in the accumulation of ECM components and thickening of the glomerular and tubular basement membranes. This causes tubulointerstitial damage, thereby resulting in tubulointerstitial fibrosis [33]. The development of diabetic nephropathy correlates with hyperglycaemia as it leads to tubulointerstitial damage through several mechanisms, including increased levels of protein kinase C (PKC), high levels of advanced glycation end-products (AGEs) and increased angiotensin II production.

Hyperglycaemia prompts an abnormal stimulation of protein kinase C (PKC), which has been linked to the development of diabetic nephropathy. Increased concentrations of PCK correlate with an intensification of fibronectin, TGF-1, and type IV collagen levels [34], demonstrating that increased PKC was detected in rats with diabetic nephropathy. A reduction was also observed in the concentration of growth factors and ECM protein when streptozotocin-induced diabetic rats were given a PKC inhibitor.

AGEs are a heterogeneous group of proteins or lipids that become glycated due to exposure to

sugar. Elevated AGE levels have been observed in various diseases, including chronic renal failure [35]. Hyperglycaemia has been reported to increase the formation of AGEs induced by oxidative stress. They are absorbed by the proximal tubular cells after being filtered by the glomerulus. AGEs lead to tubular injury by causing an increase in the concentration of TGF-β [36]. They cause glomerulosclerosis and tubulointerstitial damage through the abnormal accumulation of ECM, including collagens, by prompting the intrinsic glomerular cells to synthesise TGF-1 [37]. It was shown in a study [38] that administering ALT-711, an AGE inhibitor, to diabetic rats decreased the glomerular sclerosis index, tubulointerstitial area, and albuminuria. In addition, AGEs can enhance nucleic factor-kappa B (NFκB) activity through the activation of PCK, which, in turn, leads to tubular injury [39]. AGEs have also been linked to the progression of diabetic nephropathy as they are able to inhibit nitric oxide synthases [40]. Abnormal production of nitric oxide was found to moderate kidney function in diabetes mellitus, while it was established that a decline in kidney function related to nitric oxide deficiency [41].

Oxidative stress occurs as a result of an interaction between various molecular events due to the pathological progression of diabetic nephropathy. It is associated with the changes in the reduction-oxidation reaction (redox) state produced by chronic hyperglycaemic and AGE upregulation. These events produce chronic inflammation and glomerular tubular hypertrophy as they impact the renin-angiotensin system and TGF-β signalling. Renal fibrosis is mainly due to the build-up of mesangial cells, which supports the accumulation of ECM, glomerular and tubular membrane thickening, podocyte dysfunction, and apoptosis [42]. All of these activities are redox changes that cause the manifestation of proteinuria, albuminuria, tubulointerstitial fibrosis, and glomerulosclerosis [43].

The interaction of receptors for advanced glycation end products (RAGEs) increases the AGE metabolic signals, thereby prompting cell migration, proliferation, autophagy, and apoptosis based on the target cells [44]. Interaction between the AGEs and RAGEs activates the peroxisome proliferator-activated gamma receptor [45], which, in turn, incites the intracellular production of reactive oxygen species [35]. The signalling of redox-sensitive pathways activates transcription factors, activator protein 1 (AP-1), specificity protein 1 (SP-1), and NFκB, which induces an array of proinflammatory and profibrotic reactions.

The mRNA expression of PAI-1 is upregulated in kidney diseases that involve fibrosis and diabetic nephropathy [46]. A study [47] reported that PAI-1 mRNA expression in two types of diabetic rats was upregulated in the tubular epithelial cells. As mentioned previously, TGF-β

is induced by angiotensin II. This stimulates PAI-1 production [17] and leads to the accumulation of ECM. According to a study [48], TGF-β is a key moderator of ECM accumulation in diabetic nephropathy [20]. In cells grown in high glucose concentrations, elevated thrombospondin-1 protein expression stimulated TGF-β bioactivity, leading to greater ECM accumulation. The mRNA expression of glomerular TGF-β was shown to escalate in parallel with an increase in collagen I mRNA expression in streptozotocin-induced diabetic rats [49]. However, the extent to which collagen I and PAI-1 mRNA were expressed in this study varied.

5. Synopsis of the Main Research Outcomes

MMP-9 has been found to contribute to TIF. As stated previously, it stimulates the entire pathway for the EMT of the renal tubular cells [50, 51], leading to extreme ECM synthesis. Both a decrease and an increase in the mRNA expression of TIMP-1 and MMP-9, respectively, were demonstrated in diabetic rats in a study [52]. According to a study [53], α3β1 integrin stimulates MMP-9 expression in human and mouse keratinocytes. α3β1, α4β1, α5β1 and α6β1 integrins have been utilised in numerous studies to evaluate their ability to influence MMP-9 expression and secretion in several cell types [54-57]. αvβ3 integrins were demonstrated to be associated with the regulation of MMP-9 synthesis (downregulation) to varying degrees in a study [58], suggestive that glucose-induced variations of integrin and integrin-related function in cells grown in high glucose concentrations might be mechanistically connected to the modification of MMP-9 expression as well as secretion.

TIMP-1 and MMP-9 mRNA expression was found to be changeable over 72 hours in the current study, thereby inferring the accumulation of ECM. Although the variable expression of all the markers could reflect the natural expression of these genes in this cell model, it is more likely to be owing to the approach used as the samples were duplicated in this study, whereas they were triplicated in previous studies when the comparative Ct method was employed.

6. Conclusions

This study has shown that acidosis affects RPTEC as it increases the accumulation of all markers, possibly leading to tubulointerstitial fibrosis. Hyperglycaemia had a variable effect on the expression of the ECM genes, suggesting that hyperglycaemia may lead to an increase in the deposition of ECM and then renal failure.

7. Limitations, Implications, and Further Directions of Research

Further research is required to determine the mechanism of hyperglycaemia on the expression

of extracellular matrix proteins and matrix metalloproteinase.

Acknowledgement

I would like to extend my heartfelt gratitude to Dr. Liliana Shalamanova, for her unstinting support, guidance, patience, and advice.

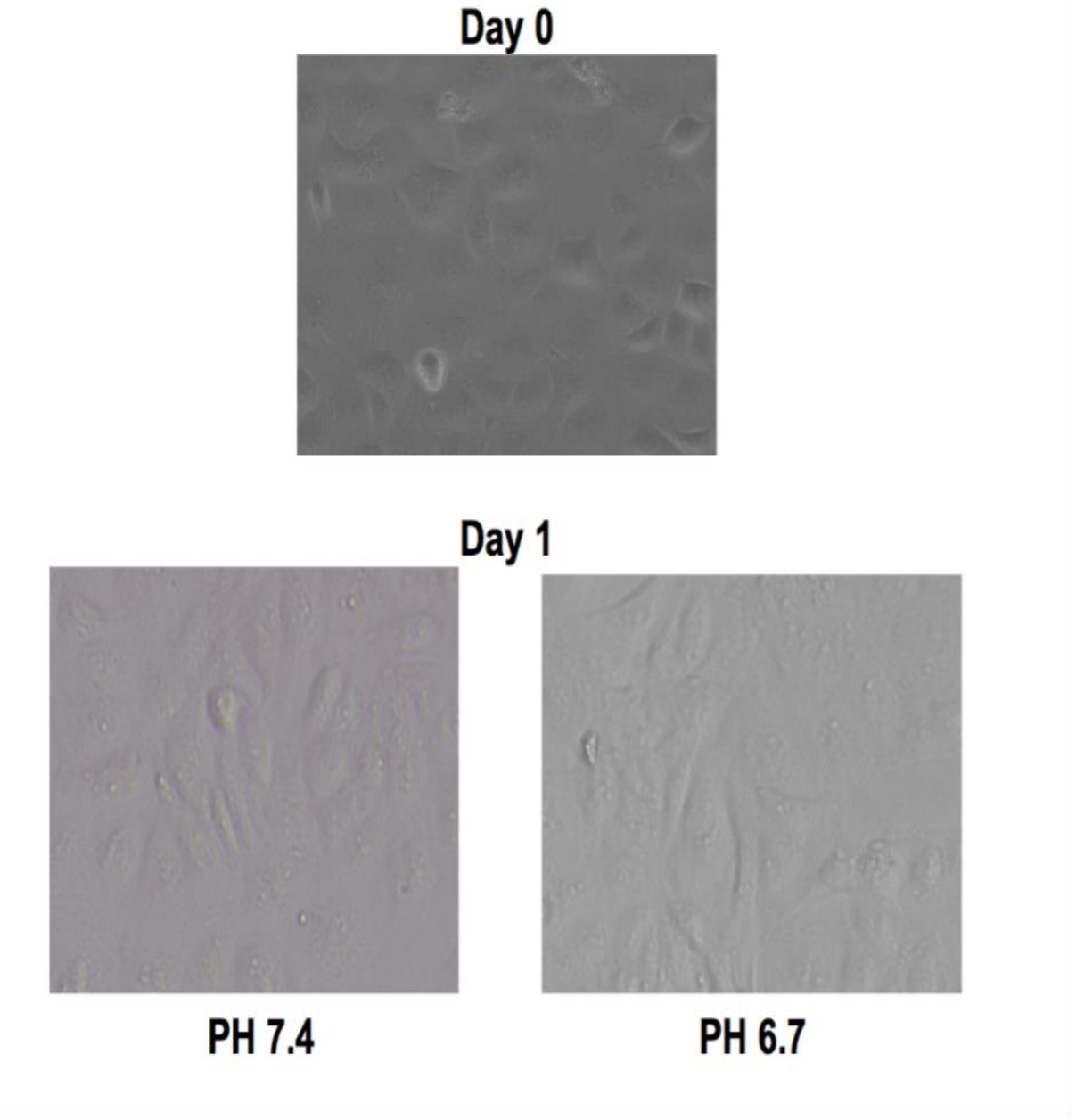

Figure 1: Cell morphology of the HK-2 cells under normal acidity (pH 7.4) and acidosis conditions (pH 6.7). The pictures were taken under 200x magnification immediately after changing the medium on (Day 0) and Day 1 (24h).

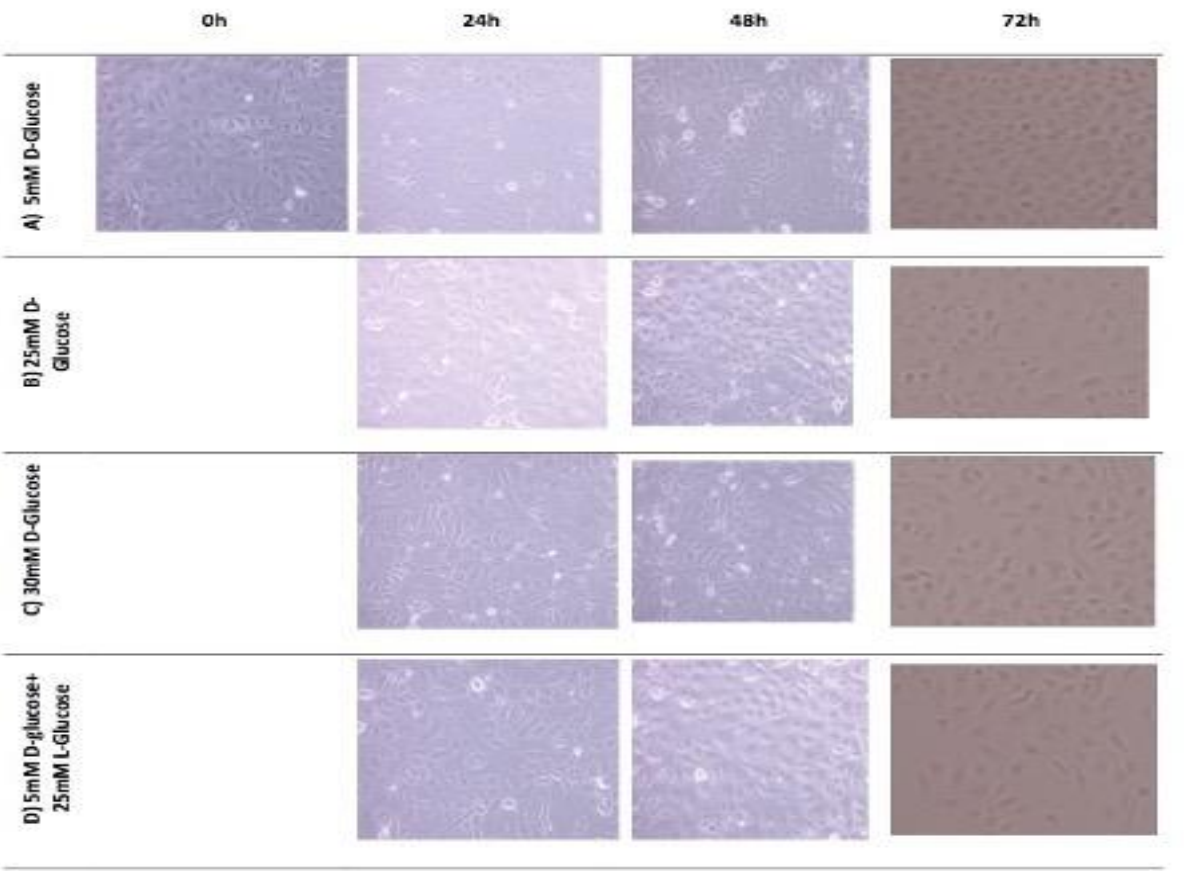

Figure 2: Cell morphology of the HK-2 cells under normal glycaemia and hyperglycemic conditions and cells exposed to an osmotic control condition. The pictures were taken under 200x magnification immediately after changing the medium (0 h) at 24h, 48h, and 72h. A) Cells exposed to 5mM D-Glucose (control); B) Cells exposed to 25mM D-Glucose (hyperglycemia); C) HK-2 cells exposed to 30mM D-Glucose (hyperglycemia); and D) HK-2 cells exposed to osmatic control (5mM D-Glucose+ 25mM L-Glucose).

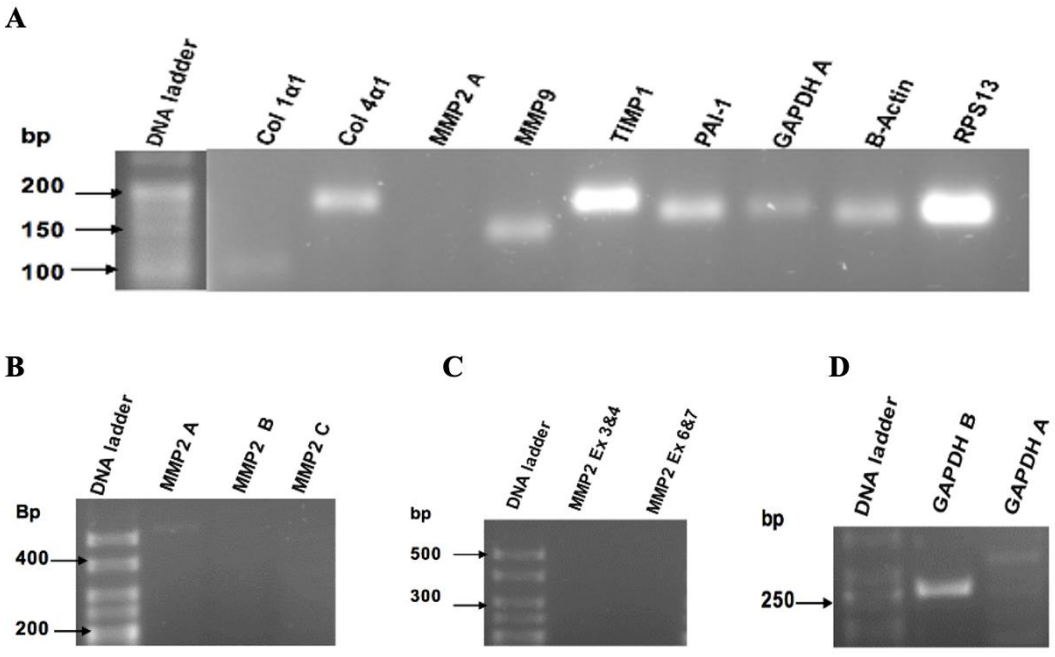

Figure 3: Primers test in 2% agarose gel electrophoresis. A) Primers Col 1α1, Col 4α1, MMP-2, MMP-9,

TIMP1, PAI-1, GAPDH β-Actin and RPS13 were tested on agarose gel electrophoresis; B) Comparison of the products of MMP-2 (A), MMP-2(B) and MMP-2(C); C) Comparison of the products of MMP-2 Ex 3&4 and MMP-2 Ex 6&7; D) Comparison of the products of GAPDH A and GAPDH B primers.

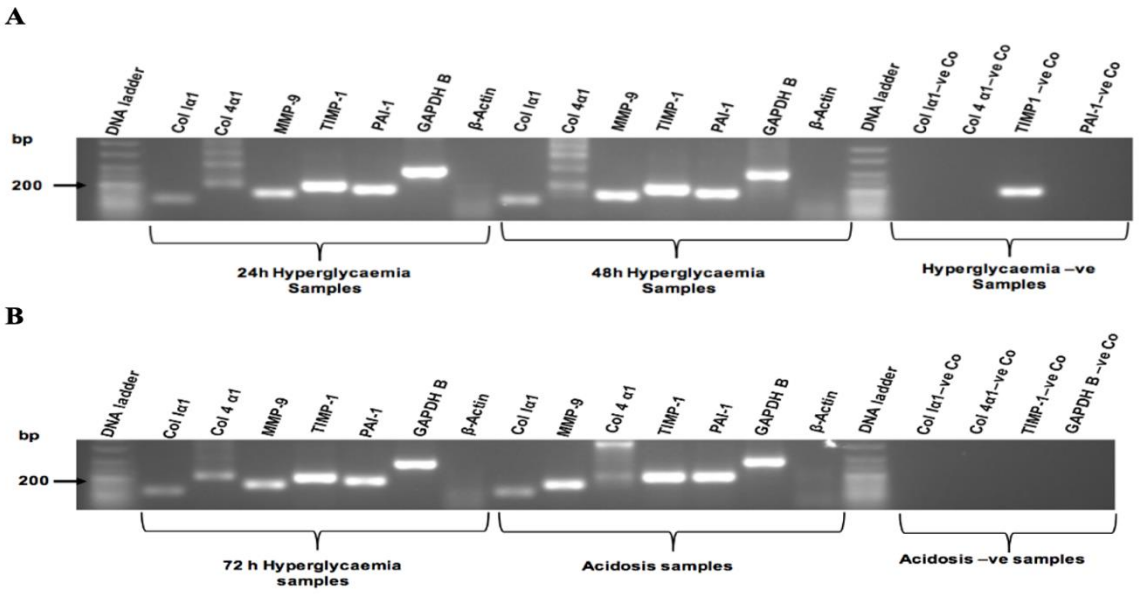

Figure 4: Agarose gel electrophoresis of the qPCR products. Samples were resolved on 2% agarose gel electrophoresis after qPCR. A) Hyperglycaemia samples at 24h and 48h and some of their negative control samples; B) Hyperglycaemia samples at 72h, acidosis samples at 24h and some of acidosis negative control samples.

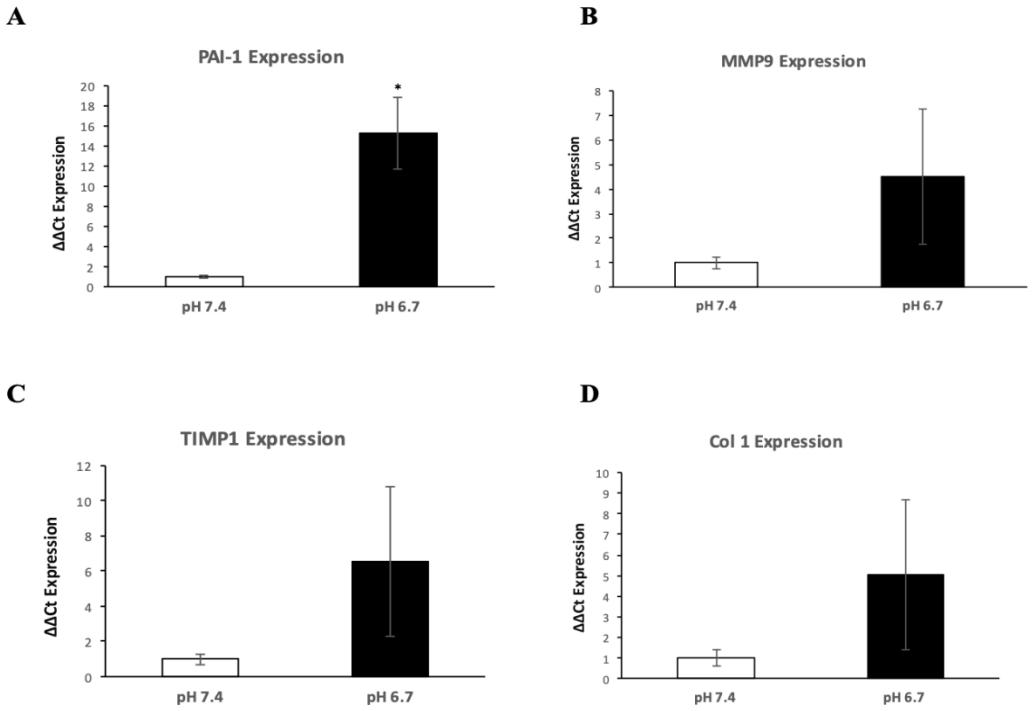

Figure 5: The effect of acidosis on the mRNA expression of ECM targets: Representative data for A) PAI-1; B) MMP-9; C) TIMP1; D) Col Iα1 (n=3) are shown. The experiment was repeated twice (n=6). Data were normalised to the GAPDH expression (*p<0.05).

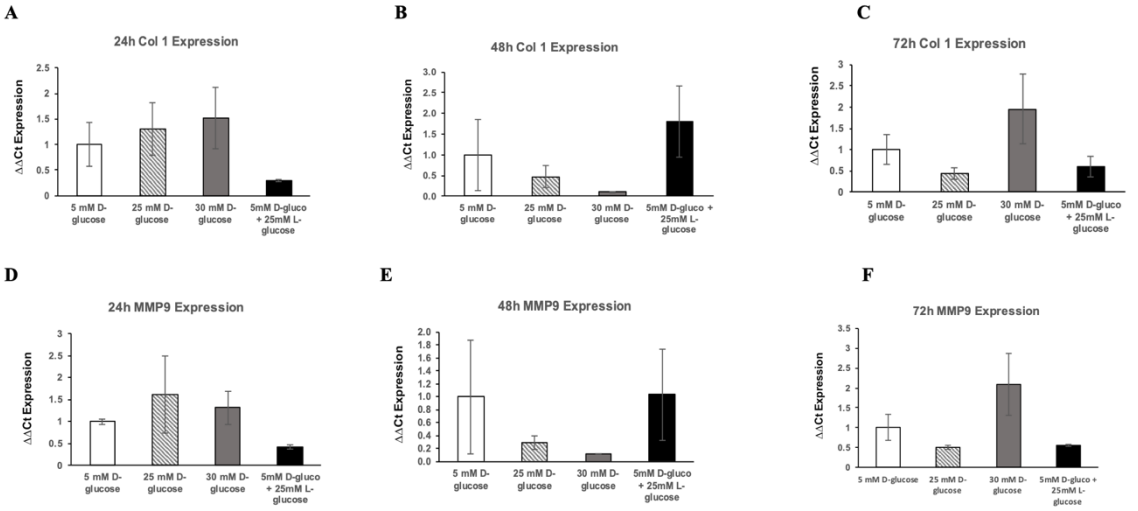

Figure 6: The effect of hyperglycaemia on mRNA expression of A) Col 1α1 at 24h; B) Col 1α1 at 48h; C) Col 1α1 at 72h; D) MMP-9 at 24h; E) MMP-9 at 48h; F) MMP-9 at 72h. Data were normalised to GAPDH expression.

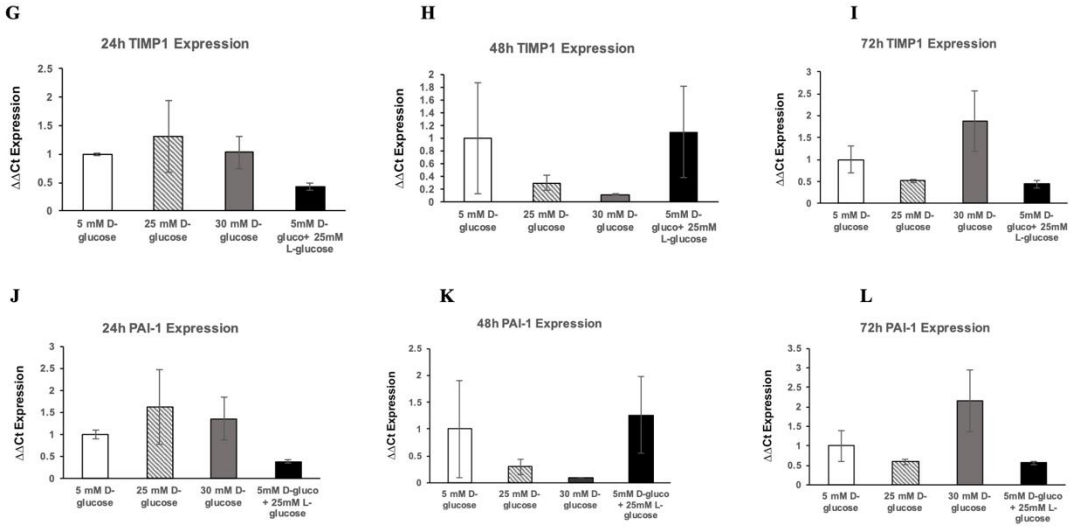

Figure 7: The effect of hyperglycaemia on mRNA expression of G) TIMP1 at 24h. H) TIMP1 at 48h. I) TIMP1 at 72h. J) PAI-1 at 24h. K) PAI-1 at 48h. L) PAI-1 at 72h. Data were normalised to GAPDH expression.

References

1. Hewitson, T.D., *Fibrosis in the kidney: is a problem shared a problem halved?* Fibrogenesis & Tissue Repair, 2012. **5**(1): p. S14.

2. Efstratiadis, G., et al., *Renal fibrosis.* Hippokratia, 2009. **13**(4): p. 224-229.

3. Kraut, J.A., *Effect of metabolic acidosis on progression of chronic kidney disease.* American Journal of Physiology - Renal Physiology, 2011. **300**(4): p. F828.

4. Kraut, J.A. and N.E. Madias, *Metabolic acidosis: pathophysiology, diagnosis and management.* Nat Rev Nephrol, 2010. **6**(5): p. 274-285.

5. Muthuppalaniappan, V.M., M. Sheaff, and M.M. Yaqoob, *Diabetic nephropathy.* Medicine, 2015. **43**(9): p. 520-525.

6. Kolset, S.O., F.P. Reinholt, and T. Jenssen, *Diabetic Nephropathy and Extracellular Matrix.* Journal of Histochemistry & Cytochemistry, 2012. **60**(12): p. 976-986.

7. Zitka, O., et al., *Matrix Metalloproteinases.* Current Medicinal Chemistry, 2010. **17**(31): p. 3751-3768.

8. Zhao, H., et al., *Matrix metalloproteinases contribute to kidney fibrosis in chronic kidney diseases.* World Journal of Nephrology, 2013. **2**(3): p. 84-89.

9. Visse, R. and H. Nagase, *Matrix Metalloproteinases and Tissue Inhibitors of Metalloproteinases: Structure, Function, and Biochemistry.* Circulation Research: Journal of the American Heart Association, 2003. **92**(8): p. 827-839.

10. Tan, T.K., et al., *Macrophage Matrix Metalloproteinase-9 Mediates Epithelial-Mesenchymal Transition in Vitro in Murine Renal Tubular Cells.* The American Journal of Pathology, 2010. **176**(3): p. 1256-1270.

11. Johnson, T.S., et al., *Matrix Metalloproteinases and Their Inhibitions in Experimental Renal Scarring.* Nephron Experimental Nephrology, 2002. **10**(3): p. 182-195.

12. Dalgleish, R., *The human type I collagen mutation database.* Nucleic Acids Research, 1997. **25**(1): p. 181-187.

13. Małgorzewicz, S., E. Skrzypczak-Jankun, and J. Jankun, *Plasminogen activator inhibitor-1 in kidney pathology (Review).* International Journal of Molecular Medicine, 2013. **31**(3): p. 503-510.

14. Cheng, Z., et al., *MMP-2 and 9 in Chronic Kidney Disease.* International Journal of Molecular Sciences, 2017. **18**(4): p. 776.

15. Baricos, W.H., et al., *Transforming growth factor-beta is a potent inhibitor of extracellular matrix degradation by cultured human mesangial cells.* Journal of the American Society of Nephrology, 1999. **10**(4): p. 790-795.

16. Krag, S., et al., *TGF-beta 1-induced glomerular disorder is associated with impaired concentrating ability mimicking primary glomerular disease with renal failure in man.* Laboratory Investigation, 2000. **80**(12): p. 1855-1868.

17. Kerins, D.M., Q. Hao, and D.E. Vaughn, *ANGIOTENSIN INDUCTION OF PAI-1 EXPRESSION IN ENDOTHELIAL-CELLS IS MEDIATED BY THE HEXAPEPTIDE ANGIOTENSIN-IV.* Journal of Clinical Investigation, 1995. **96**(5): p. 2515-2520.

18. Wesson, D.E., C.-H. Jo, and J. Simoni, *Angiotensin II receptors mediate increased distal nephron acidification caused by acid retention.* Kidney International, 2012. **82**(11): p. 1184-1194.

19. Strutz, F. and M. Zeisberg, *Renal fibroblasts and myofibroblasts in chronic kidney disease.* Journal of the American Society of Nephrology, 2006. **17**(11): p. 2992-2998.

20. Poczatek, M.H., et al., *Glucose Stimulation of Transforming Growth Factor-β Bioactivity in Mesangial Cells Is Mediated by Thrombospondin-1.* The American journal of pathology, 2000. **157**(4): p. 1353-1363.

21. Catania, J.M., G. Chen, and A.R. Parrish, *Role of matrix metalloproteinases in renal pathophysiologies.* American Journal of Physiology - Renal Physiology, 2007. **292**(3): p. F905.

22. Cai, G., et al., *Tissue inhibitor of metalloproteinase-1 exacerbated renal interstitial fibrosis through enhancing inflammation.* Nephrology Dialysis Transplantation, 2008. **23**(6): p. 1861-1875.

23. Nath, K.A., M.K. Hostetter, and T.H. Hostetter, *Pathophysiology of chronic tubulo-interstitial disease in rats. Interactions of dietary acid load, ammonia, and complement component C3.* Journal of Clinical Investigation, 1985. **76**(2): p. 667-675.

24. Halperin, M.L., J.H. Ethier, and K.S. Kamel, *Ammonium excretion in chronic metabolic acidosis: Benefits and risks.* American Journal of Kidney Diseases, 1989. **14**(4): p. 267-271.

25. Nath, K.A., M.K. Hostetter, and T.H. Hostetter, *Increased ammoniagenesis as a determinant of progressive renal injury.* American Journal of Kidney Diseases, 1991. **17**(6): p. 654-657.

26. Ortega, L.M. and S. Arora, *Metabolic acidosis and progression of chronic kidney disease: Incidence, pathogenesis, and therapeutic options.* Nefrologia, 2012. **32**(6): p. 724-730.

27. Kohan, D.E., et al., *Physiology of endothelin and the kidney.* Comprehensive Physiology, 2011. **1**(2): p. 883-919.

28. De Miguel, C., et al., *Endothelin-1 and the kidney: new perspectives and recent findings.* Current opinion in nephrology and hypertension, 2016. **25**(1): p. 35-41.

29. Ruizortega, M., et al., *INVOLVEMENT OF ANGIOTENSIN-II AND ENDOTHELIN IN MATRIX PROTEIN-PRODUCTION AND RENAL SCLEROSIS.* JOURNAL OF HYPERTENSION, 1994. **12**: p. S51-S58.

30. Remuzzi, G., *Role of endothelin in the development of glomerulosclerosis.* Kidney and Blood Pressure Research, 1996. **19**(3-4): p. 182-183.

31. Chen, W. and M.K. Abramowitz, *Metabolic acidosis and the progression of chronic kidney disease.* BMC NEPHROLOGY, 2014. **15**(1): p. 55-55.

32. Maisonneuve, P., et al., *Distribution of primary renal diseases leading to end-stage renal failure in the United States, Europe, and Australia/New Zealand: results from an international comparative study.* American journal of kidney diseases, 2000. **35**(1): p. 157-165.

33. Lassila, M., et al., *Plasminogen activator inhibitor-1 production is pathogenetic in experimental murine diabetic renal disease.* Diabetologia, 2007. **50**(6): p. 1315-1326.

34. Koya, D., et al., *Characterization of protein kinase C β isoform activation on the gene expression of transforming growth factor-β, extracellular matrix components, and prostanoids in the glomeruli of diabetic rats.* Journal of Clinical Investigation, 1997. **100**(1): p. 115-126.

35. Bohlender, J.M., et al., *Advanced glycation end products and the kidney.* American Journal of Physiology - Renal Physiology, 2005. **289**(4): p. 645-659.

36. Yamagishi, S.-I., et al., *Advanced glycation end products inhibit de novo protein synthesis and induce TGF-β overexpression in proximal tubular cells.* Kidney International, 2003. **63**(2): p. 464-473.

37. Schena, F.P. and L. Gesualdo, *Pathogenetic mechanisms of diabetic nephropathy.* Journal of the American Society of Nephrology, 2005. **16**(3): p. S30-S33.

38. Forbes, J.M., et al., *The breakdown of preexisting advanced glycation end products is associated with reduced renal fibrosis in experimental diabetes.* FASEB J 2003. **17**(12): p. 1762-1764.

39. Ha, H., et al., *Role of high glucose-induced nuclear factor-κB activation in monocyte chemoattractant protein-1 expression by mesangial cells.* Journal of the American Society of Nephrology, 2002. **13**(4): p. 894-902.

40. Verbeke, P., et al., *Inhibition of nitric oxide synthase activity by early and advanced glycation end products in cultured rabbit proximal tubular epithelial cells.* Biochimica et Biophysica Acta (BBA) - Molecular Basis of Disease, 2000. **1502**(3): p. 481-494.

41. Prabhakar, S.S., *Role of nitric oxide in diabetic nephropathy.* Alternative Medicine Review, 2004. **9**(3): p. 327.

42. Miranda-Díaz, A.G., et al., *Oxidative Stress in Diabetic Nephropathy with Early Chronic Kidney Disease.* Journal of Diabetes Research, 2016. **2016**: p. 1-7.

43. Manda, G., et al., *Redox Signaling in Diabetic Nephropathy: Hypertrophy versus Death Choices in Mesangial Cells and Podocytes.* MEDIATORS OF INFLAMMATION, 2015. **2015**: p. 1-13.

44. Lee, E.J. and J.H. Park, *Receptor for Advanced Glycation Endproducts (RAGE), Its Ligands, and Soluble RAGE: Potential Biomarkers for Diagnosis and Therapeutic Targets for Human Renal Diseases.* Genomics & Informatics, 2013. **11**(4): p. 224-229.

45. Matsui, T., et al., *Telmisartan, an Angiotensin II Type 1 Receptor Blocker, Inhibits Advanced Glycation End-product (AGE)-induced Monocyte Chemoattractant Protein-1 Expression in Mesangial Cells through Downregulation of Receptor for AGEs via Peroxisome Proliferator-activated Receptor-γ Activation.* Journal of International Medical Research, 2007. **35**(4): p. 482-489.

46. Yamamoto, T., et al., *Expression of transforming growth factor beta is elevated in human and experimental diabetic nephropathy.* Proceedings of the National Academy of Sciences, 1993. **90**(5): p. 1814-1818.

47. Hagiwara, H., et al., *Expression of type-1 plasminogen activator inhibitor in the kidney of diabetic rat models.* Thrombosis Research, 2003. **111**(4): p. 301-309.

48. Sharma, K. and F.N. Ziyadeh, *Hyperglycemia and diabetic kidney disease. The case for transforming growth factor-beta as a key mediator.* Diabetes, 1995. **44**(10): p. 1139-1146.

49. Fukui, M., et al., *ECM gene expression and its modulation by insulin in diabetic rats.* Diabetes, 1992. **41**(12): p. 1520-1527.

50. Tan, T.K., et al., *Macrophage Matrix Metalloproteinase-9 Mediates Epithelial-Mesenchymal Transition in Vitro in Murine Renal Tubular Cells.* The American journal of pathology, 2010. **176**(3): p. 1256-1270.

51. Cheng, S. and D.H. Lovett, *Gelatinase A (MMP-2) Is Necessary and Sufficient for Renal Tubular Cell Epithelial-Mesenchymal Transformation.* The American Journal of Pathology, 2003. **162**(6): p. 1937-1949.

52. McLennan, S.V., et al., *Decreased matrix degradation in diabetic nephropathy: effects of ACE inhibition on the expression and activities of matrix metalloproteinases.* Diabetologia, 2002. **45**(2): p. 268-275.

53. DiPersio, C.M., et al., *Mouse keratinocytes immortalized with large T antigen acquire alpha3beta1 integrin-dependent secretion of MMP-9/gelatinase B.* Journal of cell science, 2000. **113 (Pt 16)**: p. 2909.

54. Agrez, M., et al., *The αvβ6 integrin induces gelatinase B secretion in colon cancer cells.* International journal of cancer, 1999. **81**(1): p. 90-97.

55. Esparza, J., et al., *Fibronectin upregulates gelatinase B (MMP-9) and induces coordinated expression of gelatinase A (MMP-2) and its activator MT1-MMP (MMP-14) by human T lymphocyte cell lines. A process repressed through RAS/MAP kinase signaling pathways.* Blood, 1999. **94**(8): p. 2754-2766.

56. Sugiura, T. and F. Berditchevski, *Function of α3β1–tetraspanin protein complexes in tumor cell invasion. Evidence for the role of the complexes in production of Matrix Metalloproteinase 2 (MMP-2).* The Journal of cell biology, 1999. **146**(6): p. 1375-1389.

57. Xie, B., A. Laouar, and E. Huberman, *Fibronectin-mediated Cell Adhesion Is Required for Induction of 92-kDa Type IV Collagenase/Gelatinase (MMP-9) Gene Expression during Macrophage Differentiation THE SIGNALING ROLE OF PROTEIN KINASE C-β.* Journal of Biological Chemistry, 1998. **273**(19): p. 11576-11582.

58. Karamessinis, P.M., et al., *Proximal tubular epithelial cell integrins respond to high glucose by altered cell-matrix interactions and differentially regulate matrixin expression.* Laboratory investigation, 2002. **82**(8): p. 1081.